Neurobiology of Aging 80 (2019) 127–137

Contents lists available at ScienceDirect

Neurobiology of Aging

journal homepage: www.elsevier.com/locate/neuaging

SIRT1 protects cochlear hair cell and delays age-related hearing loss via autophagy

Jiaqi Pang [a,b,c,d,1], Hao Xiong [a,b,e,1], Yongkang Ou [a,b,e], Haidi Yang [a,b,e], Yaodong Xu [a,b], Suijun Chen [a,b,e], Lan Lai [a,b,c], Yongyi Ye [a,f], Zhongwu Su [a,b], Hanqing Lin [a,b], Qiuhong Huang [a,b,e], Xiaoding Xu [c,d,*], Yiqing Zheng [a,b,e,**]

[a] Department of Otolaryngology, Sun Yat-sen Memorial Hospital, Sun Yat-sen University, Guangzhou China
[b] Institute of Hearing and Speech-Language Science, Sun Yat-sen University, Guangzhou, China
[c] Guangdong Provincial Key Laboratory of Malignant Tumor Epigenetics and Gene Regulation, Medical Research Center, Sun Yat-Sen Memorial Hospital, Sun Yat-Sen University, Guangzhou, China
[d] RNA Biomedical Institute, Sun Yat-Sen Memorial Hospital, Sun Yat-Sen University, Guangzhou, China
[e] Department of Hearing and Speech Science, Xinhua College, Sun Yat-sen University, Guangzhou, China
[f] School of Public Health, Sun Yat-Sen University, Guangzhou, China

ARTICLE INFO

Article history:
Received 10 January 2019
Received in revised form 29 March 2019
Accepted 4 April 2019
Available online 15 April 2019

Keywords:
Age-related hearing loss
Cell death
Autophagy
SIRT1
Resveratrol

ABSTRACT

Age-related hearing loss (AHL) is typically caused by the irreversible death of hair cells (HCs). Autophagy is a constitutive pathway to strengthen cell survival under normal or stress condition. Our previous work suggested that impaired autophagy played an important role in the development of AHL in C57BL/6 mice, although the underlying mechanism of autophagy in AHL still needs to be investigated. SIRT1 as an important regulator involves in AHL and is also a regulator of autophagy. Thus, we hypothesized that the modulation between SIRT1 and autophagy contribute to HC death and the progressive hearing dysfunction in aging. In the auditory cell line HEI-OC1, SIRT1 modulated autophagosome induction because of SIRT1 deacetylating a core autophagy protein ATG9A. The deacetylation of ATG9A not only affects the autophagosome membrane formation but also acts as a sensor of endoplasmic reticulum (ER) stress inducing autophagy. Moreover, the silencing of SIRT1 facilitated cell death via autophagy inhibition, whereas SIRT1 and autophagy activation reversed the SIRT1 inhibition media cell death. Notably, resveratrol, the first natural agonist of SIRT1, altered the organ of Corti autophagy impairment of the 12-month-old C57BL/6 mice and delayed AHL. The activation of SIRT1 modulates the deacetylation status of ATG9A, which acts as a sensor of ER stress, providing a novel perspective in elucidating the link between ER stress and autophagy in aging. Because SIRT1 activation restores autophagy with reduced HC death and hearing loss, it could be used as a strategy to delay AHL.

1. Introduction

Age-related hearing loss (AHL) or presbycusis is the most common form of sensory disability in the elderly (Wilson et al., 2017). Also, it is the aging form of auditory system, with characteristics of bilateral, symmetrical, and progressive sensorineural deafness (Homans et al., 2017). Estimates suggest approximately one-third of the people aged 65 or older and two-thirds of people aged 70 or older experience AHL (Lin et al., 2011; Wilson et al., 2017). Because AHL is associated with negative consequences in communication and social life quality, it is a major factor in the progression of cognitive problems in the elderly, including depression and dementia (Gates and Mills, 2005; Homans et al., 2017; Kidd and Bao, 2012; Panza et al., 2015).

AHL is complex in that it involves both the intrinsic and extrinsic factors. Especially, environmental exposures throughout life have important effects on hearing loss in the elderly (Yamasoba et al., 2013). The most prevalent pathology of AHL is the degeneration of the peripheral and central auditory structures (Fetoni et al., 2011). The primary pathological alterations observed in the

* Corresponding author at: Sun Yat-sen Memorial Hospital, Sun Yat-sen University, 107 West Yan Jiang Road, Guangzhou 510120, China. Tel.: +8613922157362; fax: +86-20-81332115.
** Corresponding author at: Department of Otolaryngology, Sun Yat-sen Memorial Hospital and Institute of Hearing and Speech-Language Science, Sun Yat-sen University, 107 West Yan Jiang Road, Guangzhou 510120, China. Tel.: +86-20-81332566; fax: +86-20-81332115.
E-mail addresses: xuxiaod5@mail.sysu.edu.cn (X. Xu), zhengyiq@mail.sysu.edu.cn (Y. Zheng).
[1] These authors contributed equally to this work.

0197-4580/$ – see front matter © 2019 Published by Elsevier Inc.
https://doi.org/10.1016/j.neurobiolaging.2019.04.003

peripheral auditory structure cochlea was the loss of hair cell (HC), typically debuting with the outer hair cells (OHCs) of the basal cochlear regions (high frequencies) (Bao and Ohlemiller, 2010; Bowl and Dawson, 2015). The HC loss extends toward the apex and the inner hair cells (IHCs) (Ohlemiller and Gagnon, 2004). In the cochlea, the OHCs mechanically amplify sound-induced vibrations of Corti (Dallos and Fakler, 2002), whereas the IHCs signal synaptically to cochlear neuron communicate auditory information to the brain (Seal et al., 2008). In mammalian animals, the HC loss is irreversible (Jagger et al., 2014; Taylor et al., 2012) and the molecular basis of HC death in AHL is largely unknown. Therefore, there is a dire need to explore the underlying mechanism and find a way to protect the HC in the progression of AHL.

Macroautophagy, hereafter referred to as autophagy, is one of the major degradation pathways in the cell, along with the ubiquitin-proteasome system (Klionsky et al., 2016). Its key function is to remove damaged organelles and aberrant macromolecules on the lysosome pathway, thereby keeping the metabolic balance and cellular function. Common denominators in the development of age-related diseases are the inability of cells to maintain adequate metabolism, proteostasis, and organelle function (Lapierre et al., 2015). Because aging results from the accumulation of cellular damage and waste promoted by chronic stresses of small magnitude, in the life span of a cell, autophagy is required to remove cellular damage and waste. Therefore, autophagy plays a direct role for the aging process (Revuelta and Matheu, 2017). Thus, a decline in autophagic cavity is a well-known observation in aging tissue (Salminen and Kaarniranta, 2009a). Autophagy is essential for HC development, as deletion of ATG5, an essential gene for autophagy, resulted in HC degeneration and profound congenital hearing loss (Fujimoto et al., 2017). Besides, autophagy is involved in the prevention of another type of hearing loss, including neomycin-, noise-, and cisplatin-induced auditory damage (Fang and Xiao, 2014; He et al., 2017; Yang et al., 2018; Yuan et al., 2015).

In our previous study, we have found that the autophagic cavity was declined in the cochlea of aged C57BL/6 mice and the decline was associated with the activation of miR-34a (Pang et al., 2017). However, the miR-34a mechanism in blocking the autophagic flux does not adequately explain the autophagic cavity decline. We suspect that the loss of autophagy in aging not only correlates with the increasing miR-34a level but also links to some factor leading to autophagy inhibition. We have proved that the increasing miR-34a level in aging cochlea results in the deficiency of its target SIRT1 (Xiong et al., 2015). Although SIRT1 is the target of miR-34a, it had a distinct and different mechanism in modulating autophagy. An increase in miR-34a reduces the number of target gene ATG4B, an important autophagy-related gene (ATG) to inhibit LC3 conversion, that blocks the autophagy (Rothe et al., 2014).

The silencing of SIRT1 inhibits autophagy through the FoxO-mediated mechanisms (Hariharan et al., 2010; Kume et al., 2010) and the acetylation of ATG proteins (Lee et al., 2008).

Therefore, we hypothesized that the modulation between SIRT1 and autophagy may have an important role in HC death and progressive hearing dysfunction in aging. Here, we revealed that SIRT1 deficiency in auditory HCs showed autophagy impairment and cell death. The strategies aimed at rebuilding SIRT1 activity to restore autophagy may be beneficial in treating AHL.

2. Materials and methods

2.1. In vivo

2.1.1. Animals and treatment

Thirteen 2-month-old and thirteen 12-month-old C57BL/6 mice (Laboratory Animal Center, Sun Yat-sen University) were used. In addition, another sixteen 2-month-old mice were randomly divided into 2 groups after auditory brainstem response (ABR) tests. The hearing threshold of 2 groups was proven to be of no significant difference.

One group of mice were subjected to dietary supplementation with 4000 mg/kg/day of resveratrol (RSV; Sigma-Aldrich, MS, USA) added to the chow for a period of 10 months (from 2 to 12 months), whereas the other group was only fed standard chow as control. After 10 months of feeding, four 2-month-old C57BL/6 mice were compared with the old mice (the diagrammatic drawing in SI). Care and use of the animals as well as the experimental protocol were reviewed and approved by the Animal Research Committee, Sun Yat-sen University, and by the Animal Research: Reporting In Vivo Experiments guidelines.

2.1.2. Auditory brainstem response

We followed the ABR measurement procedure that has been previously described in detail (Pang et al., 2016). Thresholds were estimated by using Tucker-Davis Technologies (TDT System III, Alachua, FL, USA) hardware and software. The lowest stimulation decibel level at which a positive wave in the evoked-response trace was evident was defined and marked. All ABR measurements were conducted by the same experimenter. The ABR scores were assigned by an expert who was blinded to the treatment conditions.

2.1.3. Preparation of hair cells

The narcotized mice were sacrificed after final ABR recordings, and the cochleae were removed and fixed by immersing it in 4% paraformaldehyde in phosphate-buffered saline (PBS, pH 7.4) overnight. After fixation, 24 cochleae were immersed in 10% sodium ethylenediaminetetraacetic acid for 48 hours for cochlear surface preparation and 4 immersed for 6 days for cochlear cryosection.

2.1.4. Hair cell count

The Corti was microdissected and further rinsed in PBS. Cochlear sections were incubated in 1.5% Triton X-100 for 30 minutes at room temperature. After incubation in 10% goat serum for blocking nonspecific antibody binding for 30 minutes, 100 μL of phalloidin (Life technology, CA, USA) containing fluorescein isothiocyanate was added at 37 °C in the dark for 120 minutes, followed by incubation with 4′,6-diamidino-2-phenylindole (DAPI) (10 mg/mL; Sigma-Aldrich) for 10 minutes, and mounted on glass slides in 50% glycerol.

Samples were observed and imaged with a confocal microscope (Carl Zeiss, Germany). Images from the apex through the base of the surface preparation with DAPI-stained preparation were captured using a 40× lens. The percentage of HC loss in each 0.5 mm length of epithelium was plotted versus cochlear length as a cytocochleogram.

2.1.5. Quantitative real-time polymerase chain reaction

Total RNA was isolated using TRIzol Reagent (Invitrogen, CA, USA) according to the manufacturer's protocol, with 1 mg of total RNA reverse-transcribed using a ReverTra-Plus-TM kit (Toyobo, Osaka, Japan). Primer sequences used for amplifications were as follows—SIRT1 forward: 50-CGGCTACCGAGGTCCATATAC-30, reverse: 50-ACAATCTGCCACAGCGTCAT-30; glyceraldehyde-3-phosphate dehydrogenase forward: 50-TGAACGGGAAGCTCACTGG-30, reverse: 50-GCTTCACCACCTTCTTGATGTC-30. Complementary DNA samples were amplified using SYBR Premix Ex Taq (Tli RNaseH Plus; TaKaRa, Otsu, Japan) and detected with the Roche LightCycler 480 real-time polymerase chain reaction system. Glyceraldehyde-3-phosphate dehydrogenase was used as internal control for SIRT1 normalization.

2.1.6. Immunohistochemistry of cochlear surface preparation

The Corti was microdissected and rinsed in PBS. Cochlear sections were incubated in 1.5% Triton X-100 for 30 minutes at room temperature. After incubation in 10% goat serum for blocking nonspecific antibody binding for 30 minutes at room temperature, the samples were incubated with anti-SIRT1 (1:200; Cell Signal Technology, MA, USA), LC3B (1:200; Cell Signal Technology), or p62 (1:200; Cell Signal Technology) overnight at 4 °C, respectively. After washing 3 times (10 minutes each), the tissues were incubated with the Alexa 594-conjugated or Alexa 564-conjugated secondary antibody at a concentration of 1:200 at 4 °C overnight in the dark. After washing 3 times, tissues were incubated with 100 μL of phalloidin (Life technology) containing fluorescein isothiocyanate at 37 °C in the dark for 120 minutes. After washing 3 times, tissues were incubated with DAPI for 10 minutes. After the final wash with PBS, each tissue was divided into 3 segments (apex, middle, and base) and mounted on glass slides in 50% glycerol. Immunolabeled images were taken using a confocal microscope (Carl Zeiss).

2.1.7. Immunohistochemistry of cochlear cryosections

After an overnight incubation in 30% sucrose, the cochleae were embedded in optimal cutting temperature compound (Sakura, USA), cryosectioned at a 10 mm thickness, and stored at −20 °C. Following the immunohistochemistry protocol of the cochlear surface preparation, the cryosections were incubated with anti-SIRT1 (1:200; Cell Signal Technology) overnight at 4 °C. After washing 3 times (10 minutes each), the tissues were incubated with the Alexa 594-conjugated secondary antibody at a concentration of 1:200 at 4 °C overnight in the dark. After washing 3 times, tissues were incubated with DAPI for 10 minutes. After the final wash with PBS, each tissue was mounted on glass slides in 50% glycerol. Immunolabeled images were taken using a confocal microscope (Carl Zeiss).

2.2. In vitro

2.2.1. Cell culture of HEI-OC1 cells

The establishment and characterization of the conditionally immortalized HEI-OC1 cells were described previously (Kalinec et al., 2016). Expressions of HC-specific markers, such as Prestin, Myosin 7a, and Math1, were detected in HEI-OC1 cells. The HEI-OC1 cells (kindly provided by F. Kalinec at the House Ear Institute, Los Angeles, CA, USA) were cultured in Dulbecco's Modified Eagle's Medium (Gibco, CA, USA), supplemented with 10% fetal bovine serum (Gibco) at 33 °C under 10% CO_2 (permissive conditions). To induce starvation, cells were cultured in Dulbecco's Modified Eagle's Medium with 1% fetal bovine serum at 33 °C under 10% CO_2 (Miyazaki et al., 2015).

2.2.2. SIRT1 siRNA transfection

To examine the effect of SIRT1 on autophagy, HEI-OC1 cells were transfected with SIRT1 siRNA (siSIRT1) or a negative control (siNC) (GenePharma, Shanghai, China) at 40 nM combined with lipoRNAiMax (Life Technology) and harvested 72 hours later. As preliminary screening, the GenePharma company provided 2 sequences of siSIRT1, which we named as siSIRT1-1 and siSIRT1-2.

2.2.3. Agonists and inhibitors

Experiments were also done with RSV (5 μM; Selleck Chemicals, TX, USA), a natural-occurring polyphenol and an FDA-approved supplement to activate SIRT1. SRT1720 (0.5 μM; Selleck Chemicals), a new selective synthetic small molecule, could selectively activate SIRT1. Chloroquine (CQ, 5 μM; Sigma-Aldrich) was added to prevent fusion of autophagosomes with lysosomes to confirm the autophagy cavity. Rapamycin (RAP, 10 μM; Selleck Chemicals), a well-known mTORC1 inhibitor, is known to induce autophagy in many cells. The cells were treated with the agonists and inhibitors for 24 hours before siRNA transfection.

2.2.4. Western blot analysis

Cultured cells or tissues were lysed on ice-cold radioimmunoprecipitation assay lysis buffer (ThermoPlus, MA, USA) with 1% protease inhibitor cocktail (Selleck Chemicals) for 30 minutes and centrifuged at 12,000 × *g* at 4 °C for 30 minutes, and the supernatant was gathered. Protein concentration was determined by using the protein test dye agentia (Bio-Rad, CA, USA). Protein samples (20 μg) were loaded on sodium dodecyl sulfate polyacrylamide gel for electrophoresis and transferred to a polyvinylidene fluoride membrane (Millipore, MA, USA), which were blocked with 5% nonfat dry milk in TBS with 0.1% Tween-20.

The membranes were incubated with primary antibodies anti-LC3B, anti-p62, anti-SIRT1, or anti-β-actin (1:1000; Cell Signaling Technology, CA, USA) overnight, washed 3 times (every 10 minutes) using TBS with 0.1% Tween-20, and incubated with a proper secondary antibody (1:10,000) for 1 hour at room temperature. After extensive membrane washing, the bands of immune reactivity were illustrated through enhanced chemiluminescence (Millipore). Band intensities were measured by the densiometric test through ImageJ analysis (NIH, MD, USA), and β-actin was used as internal control.

2.2.5. Transfection of cells with fluorescence LC3

The LC3-GFP-mRFP adenoviral vectors (Ad-mRFP-GFP-LC3) were used to visualize the autophagic flux process. The tandem fluorescent-tagged LC3 reporter protein was provided by HanBio Technology Co Ltd (Shanghai, China). The vectors were transfected into HEI-OC1 cells according to the manufacturer's protocol at a multiplicity of infection of 100 for 6 hours. Observation of autophagic flux was determined after fluorescent staining by evaluating the number of green fluorescent protein (GFP) and monomeric red fluorescent protein (mRFP) puncta (puncta/cell was counted).

To explore the morphology of the autophagosome, we used the lentivirus containing LC3-GFP fusion gene to focus on LC3. The lentivirus was purchased from HanBio (Shanghai, China). The HEI-OC1 cells were transfected with lentivirus-mediated GFP-LC3 to generate LC3-GFP—expressing cells. HEI-OC1 cells infected with the recombinant lentivirus according to the manufacturer's protocol at a multiplicity of infection of 100 for 6 hours. After 48 hours, cells were positively selected by culture in the presence of puromycin for 2 weeks. Observation of autophagosome formation was determined after fluorescent staining by evaluating the number of GFP puncta (puncta/cell was counted).

2.2.6. Cell viability assay

The cell viability was measured by using Cell Counting Kit-8 (Dojindo, Japan) according to the manufacturer's instructions. HEI-OC1 cells were incubated in 96-well plates (100 μL/well), and different treatments were performed with 3 replicates. After incubation, 10 μL of Cell Counting Kit-8 solution was added in each well and the plates were incubated 2 hours in 37 °C. Cell numbers were counted by measuring the optical density (OD) value at 450 nm by a Well Scan MK3 microplate reader (Labsystems, Thermo Fisher, MA, USA), and cell viability was expressed as a percentage of the control cells.

2.2.7. Immunoprecipitation

Cells were plated at a density of 1×10^6 cells/well and cultured for 24 hours. Then, HEI-OC1 cells were transfected with siSIRT1-1 or siSIRT1-2 to silence SIRT1 for 48 hours and washed with ice-cold PBS and then lysed on ice via radioimmunoprecipitation assay lysis buffer (ThermoPlus) with 1% protease inhibitor cocktail (Selleck Chemicals). The cell lysates were incubated with anti-ATG9A

(1 μg/mL, Abcam, MA, USA) or the control normal rabbit IgG (0.5 μg/mL, Cell Signal Technology) for 2 hours at 4 °C. The complexes were pulled down with protein A-beads (Santa Cruz, CA, USA) overnight at 4 °C. The proteins were isolated by centrifugation and boiling for 5 minutes. Western blot was used to recognize the conjugated proteins. To observe the ratio of acetyl-ATG9A and ATG9A, the immunoprecipitants were assessed for the presence of Ac-K and ATG9A (1:1000; Cell Signaling Technology).

2.3. Statistical analysis

The Student *t*-test or one-way analysis of variance with the Fisher post hoc test was used for statistical analysis. Values of $p < 0.05$ were considered significant.

3. Results

3.1. SIRT1 reduction impairs autophagy in 12-month-old C57BL/6 mice with progressive hearing loss and HC loss

C57BL/6 mice, a classical AHL mouse model at different ages, were used in present study to represent a working model as it is impossible to obtain human cochlea. The ABR test is an objective electrophysiological test of hearing function to monitor the progression of AHL. The average thresholds obtained from 2-month-old mice (young mice; 31.5 ± 6.5 dB at 8 kHz, 34.8 ± 5.8 dB at 16 kHz, and 67.3 ± 10.3 dB at 32 kHz) were significantly lower than those from 12-month-old mice (old/aged mice; 75.0 ± 6.0 dB at 8 kHz, 88.8 ± 5.5 dB at 16 kHz, and 95.3 ± 3.4 dB at 32 kHz) at all tested frequencies, indicating that 12-month-old C57BL/6 mice developed a severe hearing loss (Fig. 1A). To detect whether these mice exhibit typical AHL with loss of HCs, the pattern of HCs was analyzed. There was a significant increase in OHC loss of 1.5 to 5.5 mm from apex along the cochlear epithelium in the 12-month-old mice, whereas a normal pattern of inner HCs (IHC) and OHCs were seen in the 2-month-old mice (Fig. 1B and C). Age-related IHC loss was only observed in the basal turn of the cochlea (Fig. 1B and D). The aforementioned result is in agreement with previous observation that the OHC was the first and most heavily injured by oxidative damage in aging (Jiang et al., 2007). The ABR recordings and the amount of HC loss indicated that C57BL/6 mice exhibited typical AHL in aging.

To monitor autophagy, LC3-II and p62 were used in the subsequent experiments. LC3-II serves as a widely used marker of autophagosome, whereas p62 (a selective substrate for autophagy) could be used as an index of autophagic degradation. Compared with the cochlea of 2-month-old mice, LC3B-II was reduced in that of 12-month-old mice. We further showed that levels of p62 were markedly increased in the cochlea of the old mice compared with that of the young (Fig. 1E–G).

In the Corti of the 12-month-old C57BL/6 mice, SIRT1 mRNA was significantly decreased (Fig. 1H) compared with that of the 2-month-old C57BL/6 mice. In the young group, SIRT1 protein was strongly expressed in the IHCs and OHCs but weaker in immunofluorescence, whereas in the 12-month-old mice, SIRT1 intensity was significantly weaker in the IHCs and could not be detected in the OHCs (Fig. 1I). These results suggested that in the Corti of mice with AHL, expression of SIRT1 reduced and the autophagy cavity declined with HC loss.

3.2. SIRT1 reduction impairs autophagy in HEI-OC1 cells

To examine whether SIRT1 reduction had an effect on autophagy, HEI-OC1, an auditory cell displays a variety of markers for sensory HCs, including Math1, Myosin 7a, and Prestin, was used. We investigated the status of autophagy in 2 sequences of siSIRT1. HEI-OC1 cells were transfected with either siSIRT1-1, or siSIRT1-2, or siNC as a negative control. As shown in Fig. 2C and E, the silencing effect of siSIRT1-2 was higher than siSIRT1-1 at 48 hours after the transfection. Therefore, we chose to use siSIRT1-2 for subsequent experiment. The reduction of SIRT1 significantly decreases the conversion of LC3-I to LC3-II, whereas p62 was significantly increased; this leads us to the conclusion that the reduction of SIRT1 results in autophagy impairment.

To further verify the role of SIRT1 in autophagy modulation, we enhanced the expression of SIRT1 through the addition of (1) a naturally occurring polyphenol, RSV—RSV is an FDA-approved supplement, known to activate SIRT1 and is important in attenuating cellular injury and oxidative stress (He et al., 2010; Kim et al., 2013; Wang et al., 2017)—and (2) a new selective synthetic small molecule, SRT1720, which could selectively activate SIRT1 (Fan et al., 2013). To examine the SIRT1 activation through RSV and SRT1720, SIRT1 deacetylated target ac-p53 was measured by Western blotting. The ratios of acetylated p53 to total p53 were attenuated in HEI-OC1 cells (Fig. S1A-D). Furthermore, RSV and SRT1720 increased SIRT1 expression and corrected autophagy impairment. LC3-I to LC3-II conversion was significantly increased in RSV- (Fig. 2C and D) and SRT1720- (Fig. 2E and F) treated cells, whereas p62 protein was decreased.

3.3. SIRT1 modulates autophagosome formation in HEI-OC1 cells

RAP, a well-known mTORC1 inhibitor, is known to induce autophagy in many cells. To further explore whether autophagy was regulated by SIRT1, the autophagy activation from RAP was performed in HEI-OC1 cells with the siSIRT1 transfection. The effect of siSIRT1 on autophagy was deficient, as the autophagosome marker LC3-II decreased and the autophagy degradation marker p62 increased. RAP treatment resulted in the increment of LC3-II and the loss of p62 even in the presence of siSIRT1 (Fig. 3A and B). To visualize the autophagic flux process, the tandem fluorescent-tagged LC3 reporter protein (Ad-mRFP-GFP-LC3) was transfected in HEI-OC1 cells. Generally, LC3 appears in a diffused pattern in the cytoplasm. When autophagy is activated, LC3 would be aggregated and appears in a punctate pattern. The GFP signal is sensitive to the acidic condition of the lysosome lumen, whereas mRFP is more stable. Therefore, the yellow punctum, which is the colocalization of both GFP and mRFP fluorescence, indicates a compartment that has not fused with a lysosome, such as the phagophore or an autophagosome, whereas the red punctum from an mRFP signal without GFP corresponds to an amphisome or autolysosome. The state of autophagy can be evaluated according to the number of yellow and red puncta. To better observe this phenomenon, HEI-OC1 cells were starved before the experiment to raise the autophagy level in the cell. Cells treated with siSIRT1 showed an attenuated number of yellow and red puncta in the perinuclear region and cytoplasm compared with the control. Conversely, RSV or RAP treatment could increase both yellow and red puncta compared with the siSIRT1 (Fig. 3C and D), suggesting that SIRT1 inhibition could lessen autophagosome synthesis in HEI-OC1 cells. To further monitor the autophagy, we added CQ into the cells to prevent fusion of autophagosomes with lysosomes. After CQ addition, LC3-II did not accumulate as much as cells transfected with siSIRT1, although p62 protein continued to accumulate (Fig. 3E and F), implying that the effects of CQ in autophagic fusion inhibition were abolished by the downregulation of SIRT1. Then, LC3-GFP HEI-OC1 cells were used to visualize the formation of the autophagosome. HEI-OC1 cells treated with SRT1720 showed an increased number of green puncta in the perinuclear region and cytoplasm compared with the control, whereas SRT1720 treatment with CQ showed significantly increased puncta (Fig. 3G and H). Because LC3-

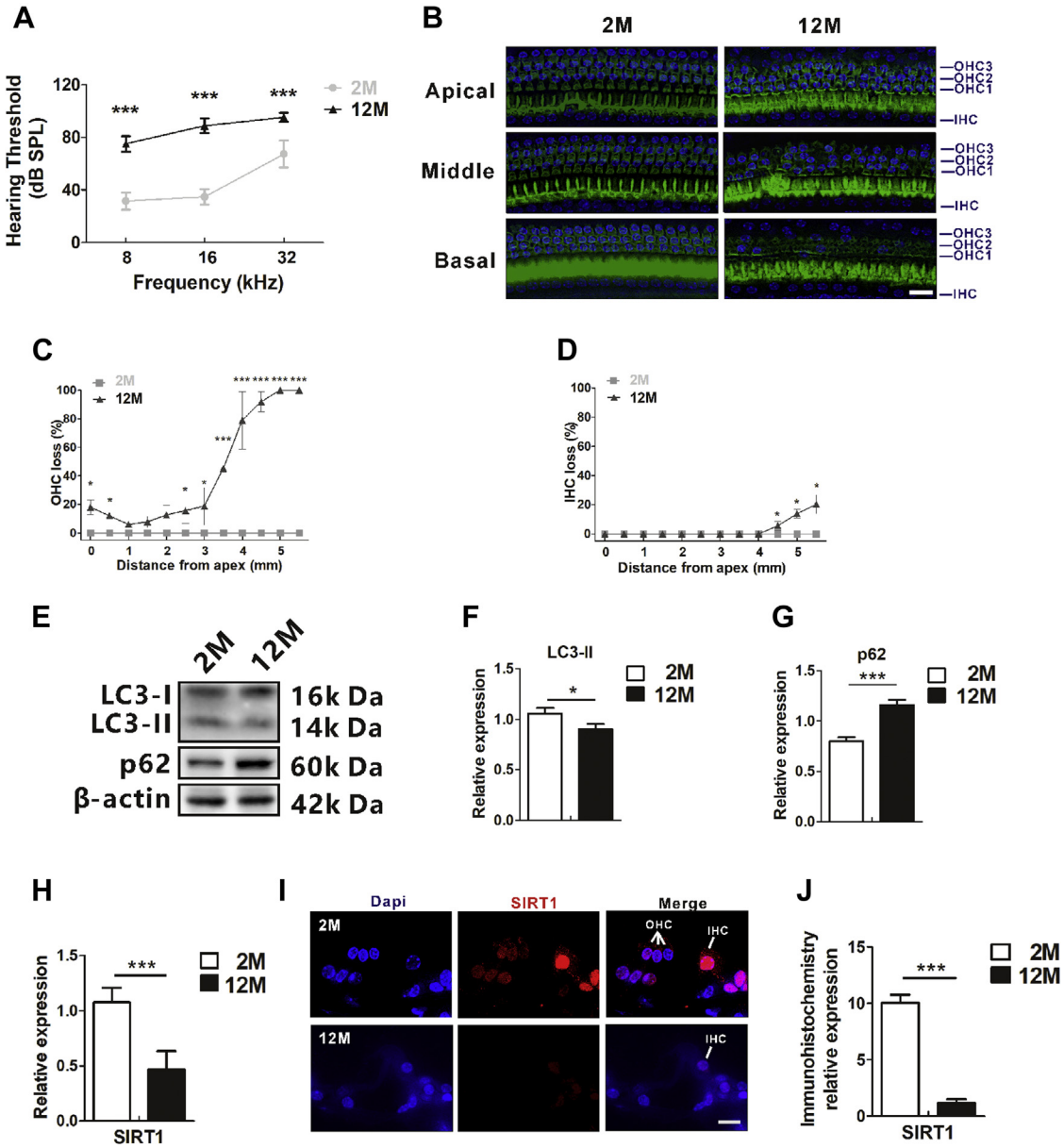

Fig. 1. SIRT1 reduction impairs autophagy in C57BL/6 mice with AHL. (A) ABR thresholds increased with aging in C57BL/6 mice at 8, 16, and 32 kHz (n = 13 mice). (B) Surface preparations were stained with DAPI (blue) and Myosin 7a as an HC marker (green). (C and D) HC counts obtained at different ages (n = 4 cochleae). (E–G) Western blots and densitometry analysis for the autophagy markers LC3-II and p62 from cochlear tissue at different ages (n = 3 independent experiments). (H) SIRT1 mRNAs were detected in qPCR of the total tissue of cochlea. (I) SIRT1 was detected in HCs. Cell nuclei were counter stained with DAPI (blue) and SIRT1 (red) (n = 4 cochleae). (J) Densitometry analysis of SIRT1 protein location for IHCs at different ages. Scale bar, 10 μm. Data represent mean ± SEM. * $p < 0.05$, *** $p < 0.001$. Abbreviations: ABR, auditory brainstem response; AHL, age-related hearing loss; HC, hair cell; OHC, outer hair cell; IHC, inner hair cell; RSV, resveratrol. (For interpretation of the references to color in this figure legend, the reader is referred to the Web version of this article.)

GFP puncta represent the formation of autophagosome, the result suggested that SIRT1 activation increased the formation of autophagosome in HEI-OC1 cells.

3.4. SIRT1 changes the deacetylation substrate of the key autophagy induction–associated protein ATG9A

The acetylation status is regarded as a critical mechanism underlying the regulation of activities of numerous autophagy machinery, which account for the regulation of autophagy. ATG9A protein is necessary for the induction of autophagy, especially as a sensor of endoplasmic reticulum (ER) stress. The acetylation of ATG9A prevents the induction of autophagy (Pehar et al., 2012). SIRT1 as a potential candidate of deacetylase may take part in the regulation of ATG9A deacetylation. We hypothesized that SIRT1 could change the acetylation levels of ATG9A.

Treatment of HEI-OC1 cells with siSIRT1-1 and siSIRT1-2 resulted in an induction of acetylation ATG9A without the expression change of ATG9A (Fig. 4A and B). These results showed that ATG9A was a deacetylation substrate of SIRT1.

3.5. SIRT1 inhibition leads to HEI-OC1 cell death via autophagy

Enhancing or inhibiting the activity of SIRT1 could help us elucidate the role of SIRT1 in the survival of HEI-OC1 cells. The cell viability results showed that HEI-OC1 cells transfected with siSIRT1

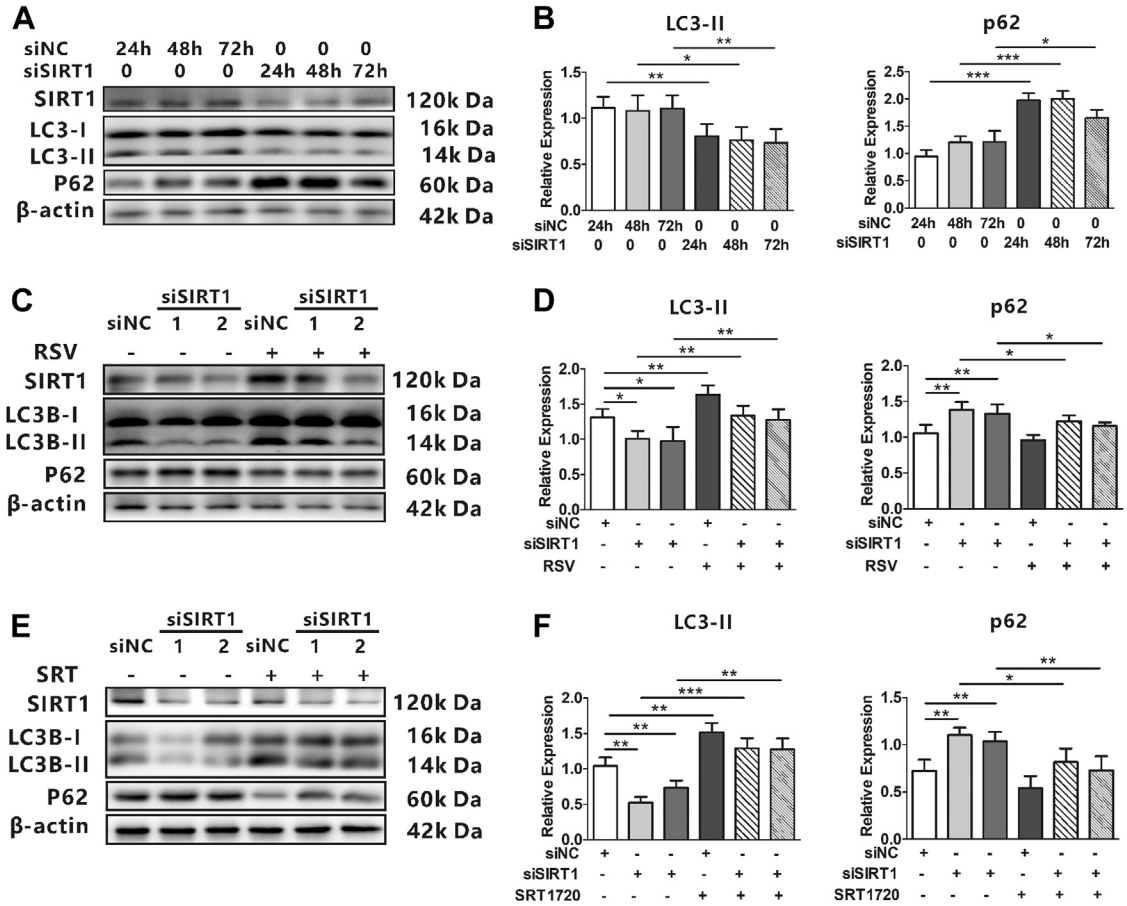

Fig. 2. SIRT1 regulates autophagy in HEI-OC1 cells. (A and B) Western blots and densitometry analysis for SIRT1 and the autophagy markers LC3-II and p62 in siSIRT1 and its control at different time points (n = 4 independent experiments). (C and D) Western blots and densitometry analysis for SIRT1 and the autophagy markers LC3-II and p62 in siSIRT1 and its control (40 nM) with or without RSV (5 μM, n = 4 independent experiments). (E and F) Western blots and densitometry analysis for SIRT1 and the autophagy markers LC3-II and p62 in siSIRT1 and its control (40 nM) with or without SRT1720 (0.5 μM, n = 4 independent experiments). Data represent mean ± SEM. * $p < 0.05$, ** $p < 0.01$, *** $p < 0.001$. Abbreviations: siSIRT1-1 and siSIRT1-2, 2 strands of siSIRT1; siNC, control of siSIRT1; RSV, resveratrol; SRT, SRT1720.

started to have a decreased survival at 24 hours compared with the controls and continued to decrease at 48 and 72 hours after transfection. Around 20%–40% cells died at 72 hours after siSIRT1 transfection (Fig. 5A). The addition of RSV could reduce cell death in SIRT1 downregulation (~20% decrease in mortality) (Fig. 5B). The protective effect of SRT1720 on cell survival was stronger than that of RSV (~20%–30% decrease in mortality; Fig. 5C), indicating that SIRT1 has protective effects on HEI-OC1 cell death. To examine whether SIRT1 expression had an effect on cell death via autophagy, an autophagy activator (RAP) and inhibitor (CQ) were used. RAP could reduce cell death in SIRT1 downregulation. Around 20%–30% of total cells were prevented from death (Fig. 5D). However, there were no significant differences between with or without CQ in siSIRT1 transfection (Fig. 5E), suggesting that the autophagy inhibitor could not aggravate cell death. Overall, SIRT1 has an effect on cell survival through autophagy regulation.

3.6. SIRT1 activation alleviates HC loss and delays AHL in C57BL/6 mice via autophagy

To demonstrate that the downregulation of SIRT1 signaling plays a major role in cochlear HC death in aged mice, we examined the effect of RSV on AHL. C57BL/6 mice aged 2 months were subjected to a period of 10 months of dietary supplementation with or without RSV at 4000 mg/kg/d, and after 12 months, in these mice, we found that RSV significantly reduced age-related auditory threshold shifts at 8, 16, and 32 kHz (Fig. 6A). There was significant alleviation of OHC loss from 1.5 to 3.5 mm from apex along the cochlear epithelium after RSV supplementation in the 12-month-old mice (Fig. 6B). However, SIRT1 restoration failed to prevent IHCs from death (Fig. 6C).

RSV supplement normalized SIRT1 expression in OHCs of the 12-month-old mice (Fig. 6D and E). RSV supplementation induced both LC3B and p62 expression in the OHCs of the 12-month-old mice to approach the healthy state of the 2-month-old mice. These results suggested that an increase in SIRT1 expression effectively restored the attenuated autophagic flux in the OHCs (Fig. 6F–I). LC3B was highly expressed in the OHCs in the cochlea of the aged mice compared with that of the young mice, which differed from the Western blot result (see Fig. 1D). However, the autophagy alteration in the total cochlear tissue and the preparations of OHCs pointed toward the same result that impaired autophagy occurred in the Corti of the 12-month-old mice. Taken together, these results supported that RSV protected OHCs by SIRT1 restoration in the induction of autophagy and delayed AHL in the 12-month-old C57BL/6 mice.

4. Discussion

SIRT1 is a family of NAD^+-dependent protein deacetylases and a particularly well-known modulator of aging. A growing body of evidence proves that SIRT1 acts against aging via reducing oxidative

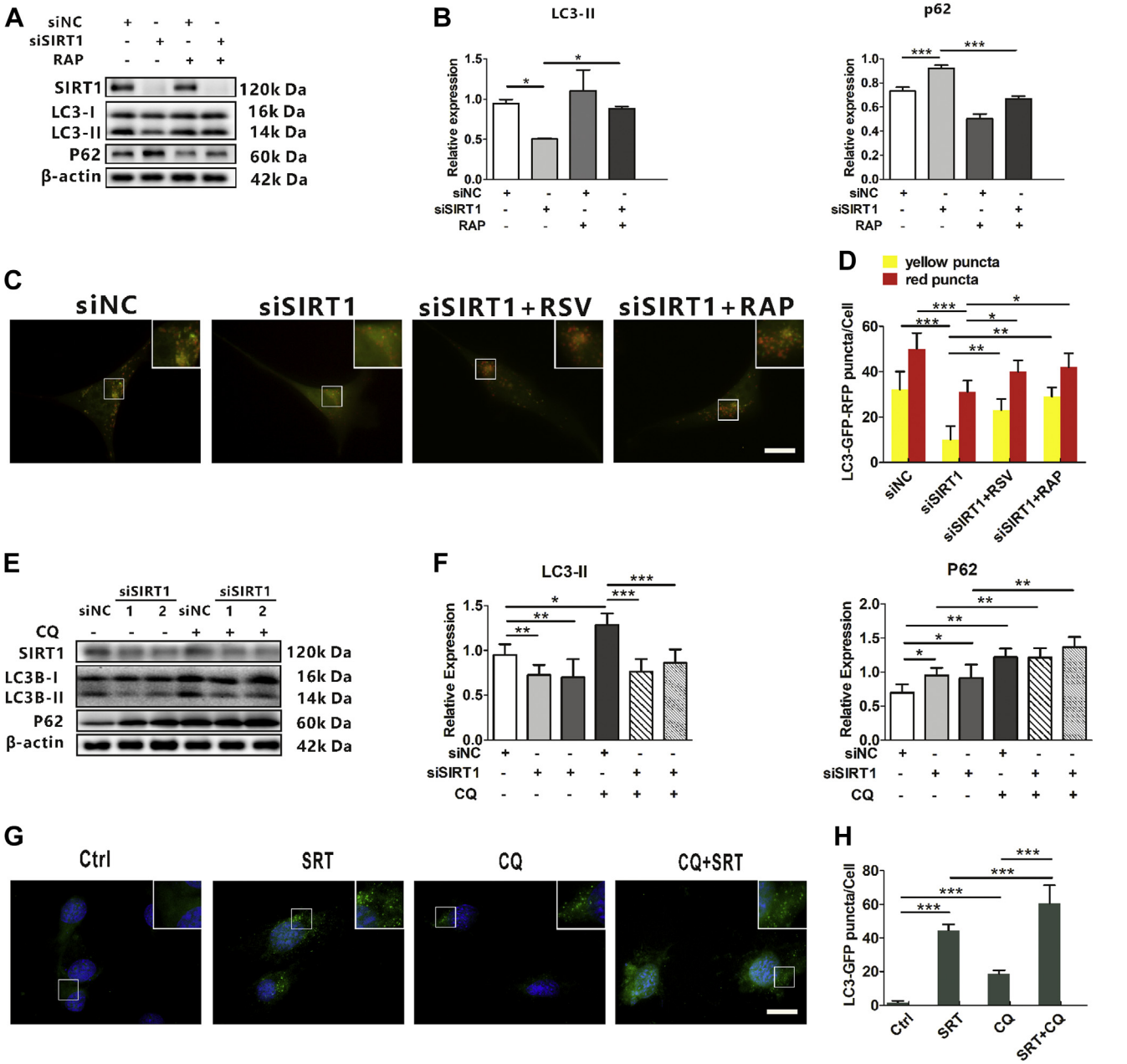

Fig. 3. SIRT1 modulates autophagosome formation in HEI-OC1 cells. (A and B) Western blots and densitometry analysis for the autophagy markers LC3-II and p62 in siSIRT1 and its control with or without RAP (10 μM, n = 3 independent experiments). (C) Fluorescence images of mRFP-GFP-LC3 in HEI-OC1 cells treated with a si-control, siSIRT1 (40 nM), siSIRT1 with RSV (5 μM), and siSIRT1 with RAP (10 μM). (D) Quantity analysis of yellow and red puncta was detected in 10 cells/experiment (n = 3 independent experiments). (E and F) Western blots and densitometry analysis for SIRT1 and the autophagy markers LC3-II and p62 in siSIRT1 and its control (40 nM) with or without CQ (5 μM, n = 5 independent experiments). (G) Fluorescence images of LC3-GFP in HEI-OC1 cells treated with SRT1720 (0.5 μM) with or without CQ (5 μM). (H) Quantity analysis of green puncta was detected in 5 cells/experiment (n = 5 independent experiments). Scale bars: 5 μm. Data represent mean ± SEM. * $p < 0.05$, ** $p < 0.01$, *** $p < 0.001$. Abbreviations: siNC, control of siSIRT1; RSV, resveratrol; RAP, rapamycin; CQ, chloroquine. (For interpretation of the references to color in this figure legend, the reader is referred to the Web version of this article.)

stress (Hasegawa et al., 2008). Besides, accumulating evidence supports SIRT1 as a key metabolic regulator was involved in a series of cellular processes associated with age-related diseases via its deacetylation of various transcription factors, such as FOXOs, p53, and NF-κB (Guarente, 2011; Herskovits and Guarente, 2014). In accordance with our previous study, the observation in current work also showed that SIRT1 expression was significantly reduced in the cochlea of aged C57BL/6 mice (Xiong et al., 2014). In addition, a recent study from the International Mouse Phenotyping Consortium showed that ABR thresholds in various frequencies were significantly increased in the young mice homozygous for a Sirt1 knockout mutation (https://www.mousephenotype.org/phenoview/?gid=363&qeid=MP:0004738&ctrl=2357729&pt=0.0001). SIRT1 regulated autophagy through different mechanisms and to respond to different insults. The activity of SIRT1 in the nucleus limits autophagy via histone deacetylation (Fullgrabe et al., 2013, 2014; Lapierre et al., 2015; Salminen and Kaarniranta, 2009b), while SIRT1-mediated deacetylation is required for autophagy induction in the cytoplasm (Lee et al., 2008; Morselli et al., 2011). In this work, HC loss and hearing loss are involved in aged C57BL/6 mice, which are accompanied by a decrease in autophagy and SIRT1 expression. The actual effect of SIRT1 in autophagy regulation

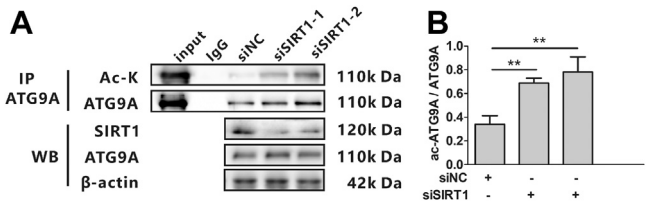

Fig. 4. SIRT1 deacetylates ATG9A in HEI-OC1 cells. (A) Acetylation levels of ATG9A were measured by IP Western blotting analysis in siSIRT1 and its control (40 nM) (n = 3 independent experiments). (B) Values were expressed as quantification of the acetylated ATG9A/total ATG9A. Data represent mean ± SEM. ** $p < 0.01$. Abbreviations: IP, immunoprecipitation; WB, Western blot; siNC, control of siSIRT1.

remains to be fully established in HC loss and AHL. In HEI-OC1 cells, the reduction of SIRT1 decreased LC3-II with a significant increment of p62. Furthermore, the silencing of SIRT1 impaired the formation of the autophagosomes when CQ and mRFP-GFP-LC3 adenoviral vectors were used to indicate the autophagic flux. These results were in accordance with the studies found in hepatic and cardiac systems that SIRT1 inhibits autophagy (Cho et al., 2017; Hariharan et al., 2010).

Protein acetylation has been recently recognized as a significant epigenetic modification that is important in controlling autophagic processes (Banreti et al., 2013). Apart from the previously known ATG5, ATG7, and ATG8 to potentiate the autophagosome formation (Lee et al., 2008) and the important transcription factor EB (TFEB) to regulate lysosomal biogenesis and autophagy degradation (Sardiello et al., 2009; Settembre et al., 2011), herein, our results indicated that SIRT1 deacetylated another autophagy protein, ATG9A, without influencing its expression. ATG9A is the only membrane-bound autophagy protein and can be used by autophagosomes from different locations, including the Golgi apparatus, the ER, and even the plasma membrane (Imai et al., 2016; Reggiori and Tooze, 2012; Webber et al., 2007). ATG9A trafficking is associated with the source of the autophagy membrane (Webber et al., 2007), However, ATG9A is retrieved from the autophagosome before fusion with the lysosome, leading to the undetectable presence of this protein on autophagosome membranes (Suzuki et al., 2007). Moreover, ATG9A acts as a sensor of the ER stress, which is often linked to autophagy (Pehar et al., 2012; Peng et al., 2018). ER stress is an important cellular stress response that is triggered by a variety of conditions that disturb cellular homeostasis. ER stress induces both autophagy and cell apoptosis (Van Erp et al., 2017), and autophagy can block apoptosis by inhibiting the activation of apoptosis-associated caspase and maintaining cellular homeostasis (Van Erp et al., 2017). The switch of the acetylation and deacetylation status of ATG9A controls the induction of autophagy under ER stress (Pehar et al., 2012). The influx of acetyl-CoA and AT-1 expression induces ATG9A acetylation, whereas in our study, SIRT1 controls the deacetylation of ATG9A. This means SIRT1 may act against the acetylation via AT-1 to regulate autophagy under ER stress.

According to our results and previous literature results, we hypothesized that in healthy cells, ER stress can induce autophagy as SIRT1 is expressed normally and ATG9A can switch from the acetylation to deacetylation status. During aging, ER stress was increased in the cochlea of the aged mice (Wang et al., 2015). AT-1 controls the inhibition of autophagy through the acetylation status of ATG9A as SIRT1 inhibition. Therefore, this study prompted a new perspective in explaining the autophagy modulation mechanism of SIRT1 and the link of ER stress to autophagy. Besides, the regulation of SIRT1 can affect the survival of HEI-OC1 cells.

Because the autophagy inhibition via CQ could not aggravate HEI-OC1 cell death, whereas the autophagy activator RAP significantly reduced cell death, we could hypothesize that SIRT1

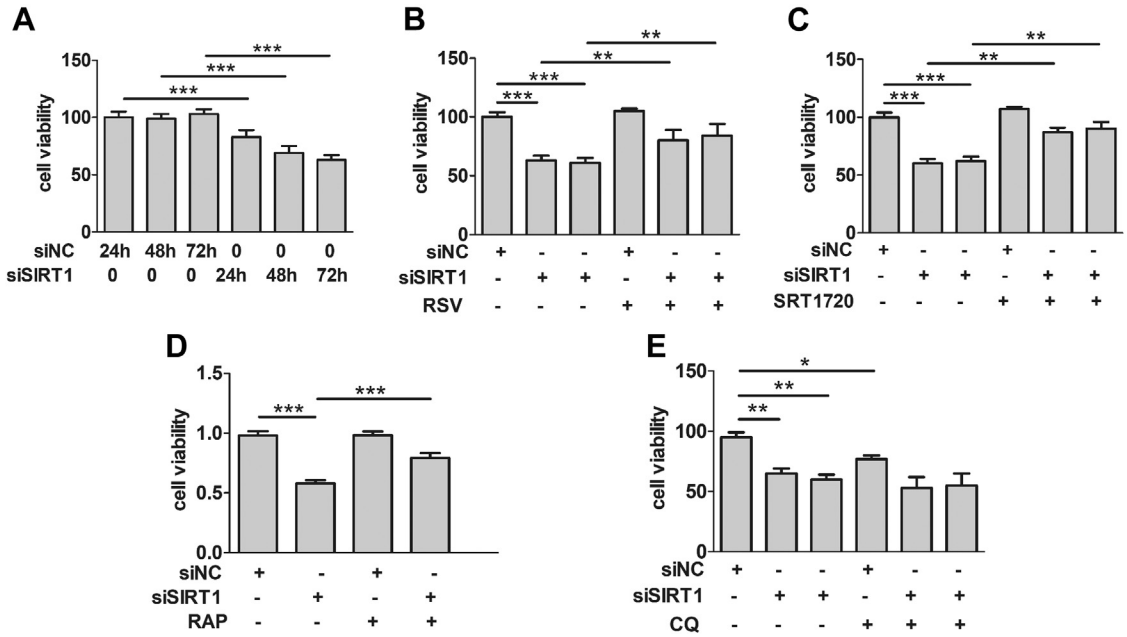

Fig. 5. SIRT1 inhibition leads to cell death via autophagy. (A) The CCK-8 assay was performed to examine cell viability of HEI-OC1 cells for siSIRT1 (40 nM) and its control at different time points after transfection (n = 3 independent experiments). (B) The CCK-8 assay was performed to examine cell viability of HEI-OC1 cells for siSIRT1 and its control (40 nM) with or without RSV (5 μM, n = 3 independent experiments). (C) The CCK-8 assay was performed to examine cell viability of HEI-OC1 cells for siSIRT1 and its control (40 nM) with or without SRT1720 (0.5 μM, n = 3 independent experiments). (D) The CCK-8 assay was performed to examine cell viability of HEI-OC1 cells for siSIRT1 and its control (40 nM) with or without RAP (10 μM, n = 3 independent experiments). (E) The CCK-8 assay was performed to examine cell viability of HEI-OC1 cells for siSIRT1 (40 nM) and its control with or without CQ (5 μM, n = 4 independent experiments). Data represent mean ± SEM. * $p < 0.05$, ** $p < 0.01$, *** $p < 0.001$. Abbreviations: siNC, control of siSIRT1; RSV, resveratrol; RAP, rapamycin; CQ, chloroquine; SRT, SRT1720.

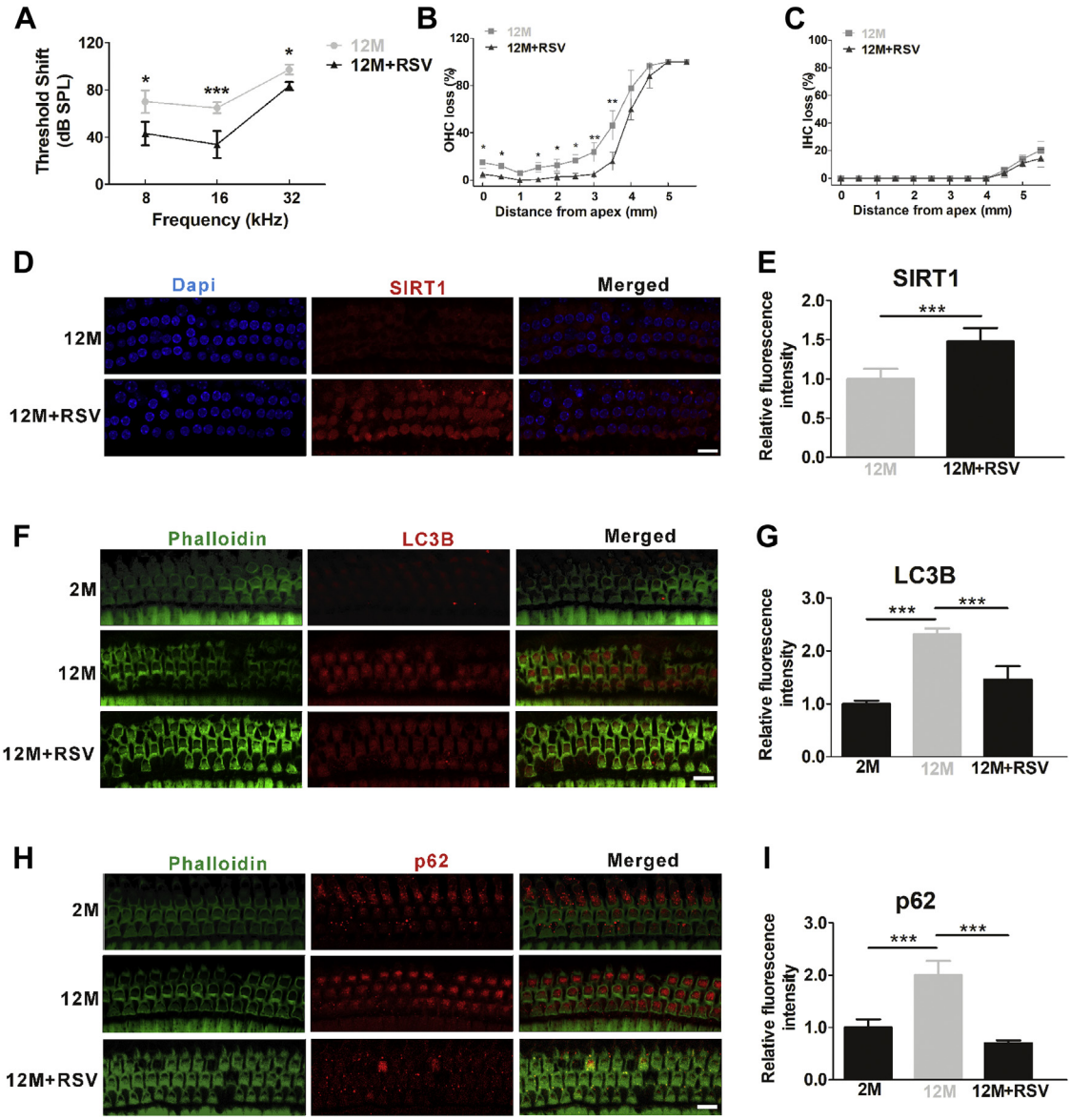

Fig. 6. Resveratrol alleviates HC loss and delays age-related hearing loss in C57BL/6 mice with autophagy recovery via SIRT1. (A) ABR thresholds decreased in RSV-treated (4000 mg/kg/d, n = 8 mice) mice compared with the same age, nontreated C57BL/6 mice at 8, 16, and 32 kHz. (B and C) HC counts obtained for the control and RSV treatment (n = right cochleae of 4 mice). (D and E) Immunohistochemical and densitometry analysis of SIRT1 protein location in OHCs for the control and RSV treatment (n = left cochleae of 4 mice). Surface preparations were stained with DAPI (blue) and SIRT1 (red). (F and G) Immunohistochemical and densitometry analysis of LC3B protein location in OHCs for the control and RSV treatment. Surface preparations were stained with phalloidin (green, located in OHC cytoplasm) and LC3B (red). (H and I) Immunohistochemical and densitometry analysis of p62 protein location in OHCs for the control and RSV treatment (right cochleae for LC3B, left cochleae of the same mice for p62, n = 4). Scale bar, 10 μm. Data represent mean ± SEM. * $p < 0.05$, ** $p < 0.01$, *** $p < 0.001$. RSV, 4000 mg/kg/d. RSV feeding started at the age of 2 months. Abbreviations: HC, hair cell; OHC, outer hair cell; IHC, inner hair cell; ABR, auditory brainstem response; RSV, resveratrol. (For interpretation of the references to color in this figure legend, the reader is referred to the Web version of this article.)

inhibition–induced autophagy impairment is correlated with cochlear HC death and might contribute to AHL. As expected, HC death and hearing loss can be reversed by RSV supplementation, which is accompanied by an increase in autophagy via SIRT1. In the cochlea of 2-month-old mice with normal ABR threshold, autophagy basal levels are very low; however, they are effective. During aging, as SIRT1 expression declines, process of autophagy gradually fails. Because the degradation of LC3B and p62 inside the autophagosome depends on the degradation of autophagy, it is not surprising that both LC3B and p62 accumulated in the OHCs of the 12-month-old mice. RSV supplementation increased the nuclear SIRT1 expression and restored the autophagy cavity presented by the reduction of LC3B and p62 accumulation. Although SIRT1 in the nucleus may limit autophagy in other organ, the effect in mice with AHL suggested that SIRT1 might be of a protective role.

It is well known that reactive oxygen species (ROS) play a major role in the development of AHL (Someya et al., 2009) because ROS production increases with age and induces oxidative damage (Balaban et al., 2005; Wallace, 2005). AHL is the response of the auditory system results from the constant small magnitude oxidative damage promoted by accumulation of ROS (Gates and Mills, 2005; Kidd and Bao, 2012; Lopez-Otin et al., 2013; Yamasoba et al., 2013). Autophagy is required in cochlea to remove exhausted and aging cells. Autophagy could suppress ROS accumulation in cells by the p62 delivery pathway (Wang et al., 2018) and its specific type mitophagy pathway (Kim et al., 2007). To promote cell

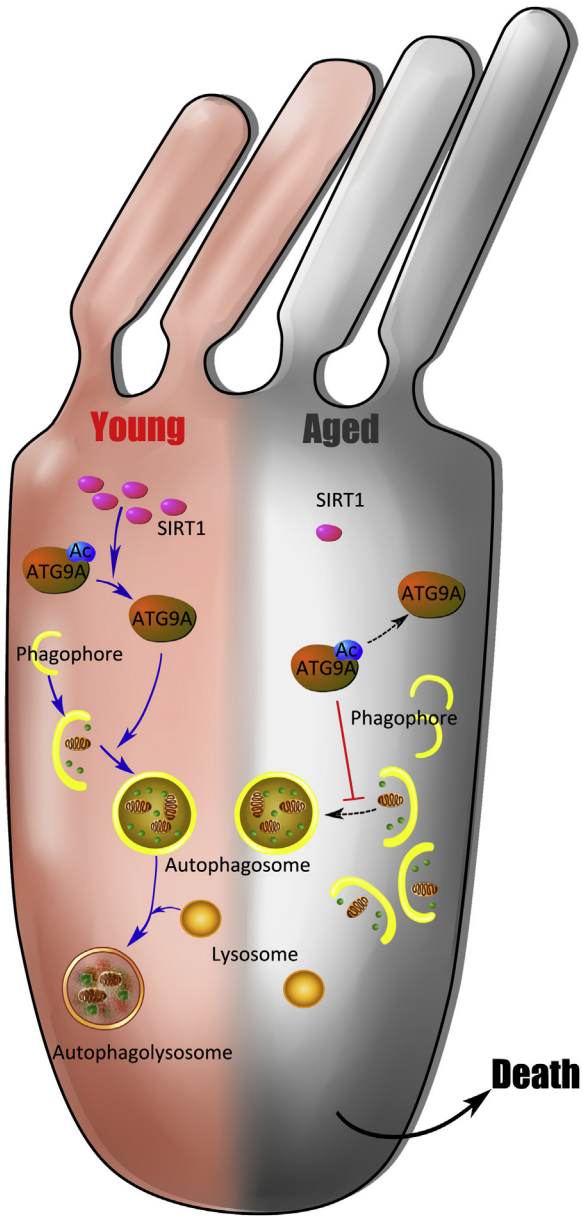

Fig. 7. Schematic model demonstrates SIRT1-modulating autophagy in hair cells of an age-related hearing loss model. Adequate SIRT1 appears in the hair cell of the young C57BL/6 mice with unobstructed autophagy as the deacetylation of ATG9A is favoring. Although in the aged C57BL/6 mice, decreased SIRT1 reduces autophagy via suppressing deacetylation of ATG9A. This leads to the hair cell death and develops to age-related hearing loss.

survival, induced autophagy can clear the aberrant biomolecules and injured organelles produced by the oxidative damage (Filomeni et al., 2015; Van Erp et al., 2017). In neomycin or gentamicin ototoxicity, it has been proven that autophagy mediates its protective effects by reducing levels of ROS (He et al., 2017). Overall, our results suggest that the SIRT1 reduction impairs autophagy, leading to ROS accumulation and cochlear functional damage in aging, implicating associated death of HCs and hearing loss. Therefore, SIRT1 activation delays AHL as SIRT1 normalizes autophagy.

Considering the fact that several substrates of SIRT1 were reported to positively regulate autophagy (Bao et al., 2016; Lee et al., 2008), our present data did not exclude the possibility that SIRT1 inhibition may promote HC loss by regulating other molecules in autophagy process. Further investigation is needed to achieve a complete understanding of the underlying mechanisms of SIRT1-mediated autophagy inhibition in HC death. Furthermore, the precise mechanism of SIRT1 in the deacetylation of ATG9A still needs to be further elucidated.

5. Conclusion

In summary in Figure 7, our study elucidated the important role of SIRT1 in maintaining autophagy function in C57BL/6 AHL mice, which accounted for HC death and progressive hearing loss. SIRT1 seems to modulate cell death through autophagy regulation in HEI-OC1 cells and takes part in the acetylation state of ATG9A, which can act as a sensor that links ER stress to autophagy. Notably, HC death and hearing loss can be reversed by the supplementation of the SIRT1 activator RSV as SIRT1 restores cochlear autophagy impairment. Taken together, these findings highlight a novel mechanism in SIRT1-induced autophagy and offer a promising therapeutic strategy in countering pathogenesis of AHL.

Disclosure

The authors have no actual or potential conflicts of interest.

Acknowledgements

This work was supported by the project funded by China Postdoctoral Science Foundation (2018M640863), the National Natural Science Foundation of China (81771018, 81570935, 81570916 and 81873699), the Guangdong Natural Science Foundation (2015 A030313041), the Guangzhou Science and Technology Foundation (2014Y2-00511), and Thousand Youth Talents Plan Project of Thousand Youth Talents. The authors thank Dr Huasong Zhang for the schematic figure illustration.

Appendix A. Supplementary data

Supplementary data associated with this article can be found, in the online version, at https://doi.org/10.1016/j.neurobiolaging.2019.04.003.

References

Balaban, R.S., Nemoto, S., Finkel, T., 2005. Mitochondria, oxidants, and aging. Cell 120, 483–495.
Banreti, A., Sass, M., Graba, Y., 2013. The emerging role of acetylation in the regulation of autophagy. Autophagy 9, 819–829.
Bao, J., Ohlemiller, K.K., 2010. Age-related loss of spiral ganglion neurons. Hear. Res. 264, 93–97.
Bao, J., Zheng, L., Zhang, Q., Li, X., Zhang, X., Li, Z., Bai, X., Zhang, Z., Huo, W., Zhao, X., Shang, S., Wang, Q., Zhang, C., Ji, J., 2016. Deacetylation of TFEB promotes fibrillar Abeta degradation by upregulating lysosomal biogenesis in microglia. Protein Cell 7, 417–433.
Bowl, M.R., Dawson, S.J., 2015. The mouse as a model for age-related hearing loss - a mini-review. Gerontology 61, 149–157.
Cho, J.H., Kim, G.Y., Pan, C.J., Anduaga, J., Choi, E.J., Mansfield, B.C., Chou, J.Y., 2017. Downregulation of SIRT1 signaling underlies hepatic autophagy impairment in glycogen storage disease type Ia. PLoS Genet. 13, e1006819.
Dallos, P., Fakler, B., 2002. Prestin, a new type of motor protein. Nat. Rev. Mol. Cell Biol. 3, 104–111.
Fan, H., Yang, H.C., You, L., Wang, Y.Y., He, W.J., Hao, C.M., 2013. The histone deacetylase, SIRT1, contributes to the resistance of young mice to ischemia/reperfusion-induced acute kidney injury. Kidney Int. 83, 404–413.
Fang, B., Xiao, H., 2014. Rapamycin alleviates cisplatin-induced ototoxicity in vivo. Biochem. Biophys. Res. Commun. 448, 443–447.
Fetoni, A.R., Picciotti, P.M., Paludetti, G., Troiani, D., 2011. Pathogenesis of presbycusis in animal models: a review. Exp. Gerontol. 46, 413–425.
Filomeni, G., De Zio, D., Cecconi, F., 2015. Oxidative stress and autophagy: the clash between damage and metabolic needs. Cell Death Differ. 22, 377–388.

Fujimoto, C., Iwasaki, S., Urata, S., Morishita, H., Sakamaki, Y., Fujioka, M., Kondo, K., Mizushima, N., Yamasoba, T., 2017. Autophagy is essential for hearing in mice. Cell Death Dis. 8, e2780.
Fullgrabe, J., Klionsky, D.J., Joseph, B., 2014. The return of the nucleus: transcriptional and epigenetic control of autophagy. Nat. Rev. Mol. Cell Biol. 15, 65–74.
Fullgrabe, J., Lynch-Day, M.A., Heldring, N., Li, W., Struijk, R.B., Ma, Q., Hermanson, O., Rosenfeld, M.G., Klionsky, D.J., Joseph, B., 2013. The histone H4 lysine 16 acetyltransferase hMOF regulates the outcome of autophagy. Nature 500, 468–471.
Gates, G.A., Mills, J.H., 2005. Presbycusis. Lancet 366, 1111–1120.
Guarente, L., 2011. Sirtuins, aging, and metabolism. Cold Spring Harb. Symp. Quant. Biol. 76, 81–90.
Hariharan, N., Maejima, Y., Nakae, J., Paik, J., Depinho, R.A., Sadoshima, J., 2010. Deacetylation of FoxO by Sirt1 plays an essential role in mediating starvation-induced autophagy in cardiac myocytes. Circ. Res. 107, 1470–1482.
Hasegawa, K., Wakino, S., Yoshioka, K., Tatematsu, S., Hara, Y., Minakuchi, H., Washida, N., Tokuyama, H., Hayashi, K., Itoh, H., 2008. Sirt1 protects against oxidative stress-induced renal tubular cell apoptosis by the bidirectional regulation of catalase expression. Biochem. Biophys. Res. Commun. 372, 51–56.
He, W., Wang, Y., Zhang, M.Z., You, L., Davis, L.S., Fan, H., Yang, H.C., Fogo, A.B., Zent, R., Harris, R.C., Breyer, M.D., Hao, C.M., 2010. Sirt1 activation protects the mouse renal medulla from oxidative injury. J. Clin. Invest. 120, 1056–1068.
He, Z., Guo, L., Shu, Y., Fang, Q., Zhou, H., Liu, Y., Liu, D., Lu, L., Zhang, X., Ding, X., Liu, D., Tang, M., Kong, W., Sha, S., Li, H., Gao, X., Chai, R., 2017. Autophagy protects auditory hair cells against neomycin-induced damage. Autophagy 13, 1884–1904.
Herskovits, A.Z., Guarente, L., 2014. SIRT1 in neurodevelopment and brain senescence. Neuron 81, 471–483.
Homans, N.C., Metselaar, R.M., Dingemanse, J.G., van der Schroeff, M.P., Brocaar, M.P., Wieringa, M.H., Baatenburg, D.J.R., Hofman, A., Goedegebure, A., 2017. Prevalence of age-related hearing loss, including sex differences, in older adults in a large cohort study. Laryngoscope 127, 725–730.
Imai, K., Hao, F., Fujita, N., Tsuji, Y., Oe, Y., Araki, Y., Hamasaki, M., Noda, T., Yoshimori, T., 2016. Atg9A trafficking through the recycling endosomes is required for autophagosome formation. J. Cell Sci. 129, 3781–3791.
Jagger, D.J., Nickel, R., Forge, A., 2014. Gap junctional coupling is essential for epithelial repair in the avian cochlea. J. Neurosci. 34, 15851–15860.
Jiang, H., Talaska, A.E., Schacht, J., Sha, S.H., 2007. Oxidative imbalance in the aging inner ear. Neurobiol. Aging 28, 1605–1612.
Kalinec, G., Thein, P., Park, C., Kalinec, F., 2016. HEI-OC1 cells as a model for investigating drug cytotoxicity. Hear. Res. 335, 105–117.
Kidd, I.A., Bao, J., 2012. Recent advances in the study of age-related hearing loss: a mini-review. Gerontology 58, 490–496.
Kim, I., Rodriguez-Enriquez, S., Lemasters, J.J., 2007. Selective degradation of mitochondria by mitophagy. Arch. Biochem. Biophys. 462, 245–253.
Kim, M.Y., Lim, J.H., Youn, H.H., Hong, Y.A., Yang, K.S., Park, H.S., Chung, S., Ko, S.H., Shin, S.J., Choi, B.S., Kim, H.W., Kim, Y.S., Lee, J.H., Chang, Y.S., Park, C.W., 2013. Resveratrol prevents renal lipotoxicity and inhibits mesangial cell glucotoxicity in a manner dependent on the AMPK-SIRT1-PGC1alpha axis in db/db mice. Diabetologia 56, 204–217.
Klionsky, D., Abdelmohsen, K., Abe, A., Abedin, M., Abeliovich, H., Acevedo Arozena, A., Adachi, H., Adams, C., 2016. Guidelines for the use and interpretation of assays for monitoring autophagy (3rd edition). Autophagy 12, 1–222.
Kume, S., Uzu, T., Horiike, K., Chin-Kanasaki, M., Isshiki, K., Araki, S., Sugimoto, T., Haneda, M., Kashiwagi, A., Koya, D., 2010. Calorie restriction enhances cell adaptation to hypoxia through Sirt1-dependent mitochondrial autophagy in mouse aged kidney. J. Clin. Invest. 120, 1043–1055.
Lapierre, L.R., Kumsta, C., Sandri, M., Ballabio, A., Hansen, M., 2015. Transcriptional and epigenetic regulation of autophagy in aging. Autophagy 11, 867–880.
Lee, I.H., Cao, L., Mostoslavsky, R., Lombard, D.B., Liu, J., Bruns, N.E., Tsokos, M., Alt, F.W., Finkel, T., 2008. A role for the NAD-dependent deacetylase Sirt1 in the regulation of autophagy. Proc. Natl. Acad. Sci. U. S. A. 105, 3374–3379.
Lin, F.R., Niparko, J.K., Ferrucci, L., 2011. Hearing loss prevalence in the United States. Arch. Intern. Med. 171, 1851–1852.
Lopez-Otin, C., Blasco, M.A., Partridge, L., Serrano, M., Kroemer, G., 2013. The hallmarks of aging. Cell 153, 1194–1217.
Miyazaki, S., Kakutani, K., Yurube, T., Maeno, K., Takada, T., Zhang, Z., Kurakawa, T., Terashima, Y., Ito, M., Ueha, T., Matsushita, T., Kuroda, R., Kurosaka, M., Nishida, K., 2015. Recombinant human SIRT1 protects against nutrient deprivation-induced mitochondrial apoptosis through autophagy induction in human intervertebral disc nucleus pulposus cells. Arthritis Res. Ther. 17, 253.
Morselli, E., Marino, G., Bennetzen, M.V., Eisenberg, T., Megalou, E., Schroeder, S., Cabrera, S., Benit, P., Rustin, P., Criollo, A., Kepp, O., Galluzzi, L., Shen, S., Malik, S.A., Maiuri, M.C., Horio, Y., Lopez-Otin, C., Andersen, J.S., Tavernarakis, N., Madeo, F., Kroemer, G., 2011. Spermidine and resveratrol induce autophagy by distinct pathways converging on the acetylproteome. J. Cell Biol. 192, 615–629.
Ohlemiller, K.K., Gagnon, P.M., 2004. Cellular correlates of progressive hearing loss in 129S6/SvEv mice. J. Comp. Neurol. 469, 377–390.
Pang, J., Xiong, H., Lin, P., Lai, L., Yang, H., Liu, Y., Huang, Q., Chen, S., Ye, Y., Sun, Y., Zheng, Y., 2017. Activation of miR-34a impairs autophagic flux and promotes cochlear cell death via repressing ATG9A: implications for age-related hearing loss. Cell Death Dis. 8, e3079.
Pang, J., Xiong, H., Yang, H., Ou, Y., Xu, Y., Huang, Q., Lai, L., Chen, S., Zhang, Z., Cai, Y., Zheng, Y., 2016. Circulating miR-34a levels correlate with age-related hearing loss in mice and humans. Exp. Gerontol. 76, 58–67.
Panza, F., Solfrizzi, V., Logroscino, G., 2015. Age-related hearing impairment-a risk factor and frailty marker for dementia and AD. Nat. Rev. Neurol. 11, 166–175.
Pehar, M., Jonas, M.C., Hare, T.M., Puglielli, L., 2012. SLC33A1/AT-1 protein regulates the induction of autophagy downstream of IRE1/XBP1 pathway. J. Biol. Chem. 287, 29921–29930.
Peng, Y., Shapiro, S.L., Banduseela, V.C., Dieterich, I.A., Hewitt, K.J., Bresnick, E.H., Kong, G., Zhang, J., Schueler, K.L., Keller, M.P., Attie, A.D., Hacker, T.A., Sullivan, R., Kielar-Grevstad, E., Arriola, A.S., Lamming, D.W., Anderson, R.M., Puglielli, L., 2018. Increased transport of acetyl-CoA into the endoplasmic reticulum causes a progeria-like phenotype. Aging Cell 17, e12820.
Reggiori, F., Tooze, S.A., 2012. Autophagy regulation through Atg9 traffic. J. Cell Biol. 198, 151–153.
Revuelta, M., Matheu, A., 2017. Autophagy in stem cell aging. Aging Cell 16, 912–915.
Rothe, K., Lin, H., Lin, K.B., Leung, A., Wang, H.M., Malekesmaeili, M., Brinkman, R.R., Forrest, D.L., Gorski, S.M., Jiang, X., 2014. The core autophagy protein ATG4B is a potential biomarker and therapeutic target in CML stem/progenitor cells. Blood 123, 3622–3634.
Salminen, A., Kaarniranta, K., 2009a. Regulation of the aging process by autophagy. Trends Mol. Med. 15, 217–224.
Salminen, A., Kaarniranta, K., 2009b. SIRT1: regulation of longevity via autophagy. Cell. Signal. 21, 1356–1360.
Sardiello, M., Palmieri, M., di Ronza, A., Medina, D.L., Valenza, M., Gennarino, V.A., Di Malta, C., Donaudy, F., Embrione, V., Polishchuk, R.S., Banfi, S., Parenti, G., Cattaneo, E., Ballabio, A., 2009. A gene network regulating lysosomal biogenesis and function. Science 325, 473–477.
Seal, R.P., Akil, O., Yi, E., Weber, C.M., Grant, L., Yoo, J., Clause, A., Kandler, K., Noebels, J.L., Glowatzki, E., Lustig, L.R., Edwards, R.H., 2008. Sensorineural deafness and seizures in mice lacking vesicular glutamate transporter 3. Neuron 57, 263–275.
Settembre, C., Di Malta, C., Polito, V.A., Garcia, A.M., Vetrini, F., Erdin, S., Erdin, S.U., Huynh, T., Medina, D., Colella, P., Sardiello, M., Rubinsztein, D.C., Ballabio, A., 2011. TFEB links autophagy to lysosomal biogenesis. Science 332, 1429–1433.
Someya, S., Xu, J., Kondo, K., Ding, D., Salvi, R.J., Yamasoba, T., Rabinovitch, P.S., Weindruch, R., Leeuwenburgh, C., Tanokura, M., Prolla, T.A., 2009. Age-related hearing loss in C57BL/6J mice is mediated by Bak-dependent mitochondrial apoptosis. Proc. Natl. Acad. Sci. U. S. A. 106, 19432–19437.
Suzuki, K., Kubota, Y., Sekito, T., Ohsumi, Y., 2007. Hierarchy of Atg proteins in pre-autophagosomal structure organization. Genes Cells 12, 209–218.
Taylor, R.R., Jagger, D.J., Forge, A., 2012. Defining the cellular environment in the organ of Corti following extensive hair cell loss: a basis for future sensory cell replacement in the Cochlea. PLoS One 7, e30577.
Van Erp, A.C., Hoeksma, D., Rebolledo, R.A., Ottens, P.J., Jochmans, I., Monbaliu, D., Pirenne, J., Leuvenink, H., Decuypere, J.P., 2017. The crosstalk between ROS and autophagy in the field of transplantation medicine. Oxid. Med. Cell. Longev. 2017, 7120962.
Wallace, D.C., 2005. A mitochondrial paradigm of metabolic and degenerative diseases, aging, and cancer: a dawn for evolutionary medicine. Annu. Rev. Genet. 39, 359–407.
Wang, W., Sun, Y., Chen, S., Zhou, X., Wu, X., Kong, W., Kong, W., 2015. Impaired unfolded protein response in the degeneration of cochlea cells in a mouse model of age-related hearing loss. Exp. Gerontol. 70, 61–70.
Wang, X., Meng, L., Zhao, L., Wang, Z., Liu, H., Liu, G., Guan, G., 2017. Resveratrol ameliorates hyperglycemia-induced renal tubular oxidative stress damage via modulating the SIRT1/FOXO3a pathway. Diabetes Res. Clin. Pract. 126, 172–181.
Wang, Y., Mandal, A.K., Son, Y.O., Pratheeshkumar, P., Wise, J., Wang, L., Zhang, Z., Shi, X., Chen, Z., 2018. Roles of ROS, Nrf2, and autophagy in cadmium-carcinogenesis and its prevention by sulforaphane. Toxicol. Appl. Pharmacol. 353, 23–30.
Webber, J.L., Young, A.R., Tooze, S.A., 2007. Atg9 trafficking in Mammalian cells. Autophagy 3, 54–56.
Wilson, B.S., Tucci, D.L., Merson, M.H., O'Donoghue, G.M., 2017. Global hearing health care: new findings and perspectives. Lancet 390, 2503–2515.
Xiong, H., Dai, M., Ou, Y., Pang, J., Yang, H., Huang, Q., Chen, S., Zhang, Z., Xu, Y., Cai, Y., Liang, M., Zhang, X., Lai, L., Zheng, Y., 2014. SIRT1 expression in the cochlea and auditory cortex of a mouse model of age-related hearing loss. Exp. Gerontol. 51, 8–14.
Xiong, H., Pang, J., Yang, H., Dai, M., Liu, Y., Ou, Y., Huang, Q., Chen, S., Zhang, Z., Xu, Y., Lai, L., Zheng, Y., 2015. Activation of miR-34a/SIRT1/p53 signaling contributes to cochlear hair cell apoptosis: implications for age-related hearing loss. Neurobiol. Aging 36, 1692–1701.
Yamasoba, T., Lin, F.R., Someya, S., Kashio, A., Sakamoto, T., Kondo, K., 2013. Current concepts in age-related hearing loss: epidemiology and mechanistic pathways. Hear. Res. 303, 30–38.
Yang, Q., Sun, G., Yin, H., Li, H., Cao, Z., Wang, J., Zhou, M., Wang, H., Li, J., 2018. PINK1 protects auditory hair cells and spiral ganglion neurons from cisplatin-induced ototoxicity via inducing autophagy and inhibiting JNK signaling pathway. Free Radic. Biol. Med. 120, 342–355.
Yuan, H., Wang, X., Hill, K., Chen, J., Lemasters, J., Yang, S.M., Sha, S.H., 2015. Autophagy attenuates noise-induced hearing loss by reducing oxidative stress. Antioxid. Redox Signal. 22, 1308–1324.